XL CILAMCE
IBERO-LATIN AMERICAN CONGRESS ON COMPUTATIONAL METHODS IN ENGINEERING
NOVEMBER 11-14, 2019
Praiamar Natal Hotel & Convention
Natal, RN-BRAZIL

# DYNAMIC ANALYSIS OF THICK CURVED BEAMS WITH THE GENERALIZED FINITE ELEMENT METHOD

**Ramon Macedo Corrêa**
*ramoncorrea1992@gmail.com*
**Marcos Arndt**
*arndt@ufpr.br*
**Roberto Dalledone Machado**
*rdm@ufpr.br*
*Graduate Program in Numerical Methods in Engineering, Federal University of Paraná*
*Curitiba, 81.531-980, Paraná, Brazil.*

**Abstract.** The traditional Finite Element Method (FEM) is widely applied in the dynamic analysis of structures, but, mostly, for higher frequencies, a great computational effort is required. In order to decrease this computational effort, the Generalized Finite Element Method (GFEM) arise as an alternative. The GFEM is based on the Partition of Unity Method and it has as its main characteristic the ability to incorporate aspects of the problem solution into the approximation space, which may decrease the computational effort involved. The curved beam element has received much attention from researchers for two main reasons: firstly, because it is a very efficient structural element that can span large distances; and secondly because it provides insight into various aspects of shell element behavior. The curved beam element is very sensitive to membrane and shear locking. In order to avoid these issues, trigonometric functions are used to expand the traditional FEM approximation space using the GFEM approach. In this paper the application of the GFEM for modal and transient analysis of thick curved beams is proposed. The GFEM results are compared to reference solutions found in literature and traditional FEM results.

**Keywords:** Thick Curved Beams, Dynamic Analysis, Generalized Finite Element Method.

## 1 Introduction

The Finite Element Method (FEM) has been successfully applied in dynamic analysis but the traditional $h$-version of the method, when looking for higher frequencies, requires a higher computational effort (Arndt et al. [1]). On the other hand, the polynomial $p$ FEM refinement presents convergence rates greater than $h$-version but high-order polynomials can result in an ill conditioned (Leung and Chan [2] and Ribeiro [3]).

In recent years, some enrichment methods based on the FEM have been developed, seeking to increase the accuracy of the solutions with lower computational effort. In this context, the Generalized Finite Element Method (GFEM) arises.

The GFEM was developed by several authors: Melenk and Babuska [4]; Duarte and Oden [5]; Oden et al. [6]; Duarte et al. [7] and Babuska et al. [8]. The method uses the Partition of Unity Method (PUM) concepts to expand the traditional FEM approximation space, using a previously knowledge about the expected solution. The GFEM has been successfully applied to dynamics analysis as shown in Arndt et al. [1], Arndt et al. [9], Torii and Machado [10], Shang et al. [11] and Weinhardt et al. [12]. The works also show some issues with the GFEM, such as the mass matrix condition number accentuated growth, that may cause numerical instability of the solution.

According to Leung and Zhu [13], the interest of researchers in curved beam elements has been increased for two main reasons: the first is the increased use of such structural element and the second is that the understanding of its behavior provides a view of various aspects of shell elements behavior. Some studies about finite elements for thin and thick curved beams, mostly to free vibration analisys, are found in the literature.

Petyt and Fleischer [14] proposed a thin curved beam element with two nodes and some alternatives of shape functions using polynomials and trigonometric functions. The use of higher order polynomials in order to describe the displacement fields was proposed by Dawe [15] for static problems and by Raveendranath et al. [16] for free vibration analysis of thin curved beams.

Rossi and Laura [17] presented a free vibration analysis of a cantilever arch with non-uniform cross-sectional area using a FEM formulation of thick curved beam. Auciello and De Rosa [18] presented a comparison between some approximated methods such as the Ritz Method, the Rayleigh-Schmidt Method, the Galerkin Method and the Finite Element Method for free vibration of arches, also using a thick curved beam formulation.

A two node element was presented by Raveendranath et al. [19], while a three node element, both for thick curved beams in static problems, was proposed by Raveendranath et al. [20]. A four node $C^0$ finite element for free vibration analysis of thick curved beam with constant and variable curvatures was proposed by Yang et al. [21].

Leung and Zhu [13] proposed an enrichment method based on the FEM, called Fourier $p$-Elements, for thin and thick curved beams. This approach uses trigonometric functions to expand the traditional FEM approximation space.

In this paper the use of the GFEM, with trigonometric enrichment, for modal and transient analysis of thick curved beam element is proposed. The solutions are compared to reference solutions found in literature and to the FEM.

## 2 Thick Curved Beam Formulation

The thick curved beam formulation is presented by Leung and Zhu [13], Raveendranath et al. [16], Raveendranath et al. [20] and Yang et al. [21]. In this formulation the effects of the shear strain are considered. The energy parcels are described by the tangential displacement ($u$), the radial displacement ($w$) and the rotation of the cross-section ($\theta$) in curvilinear coordinate system $s$-$z$, as shown in Fig. 1

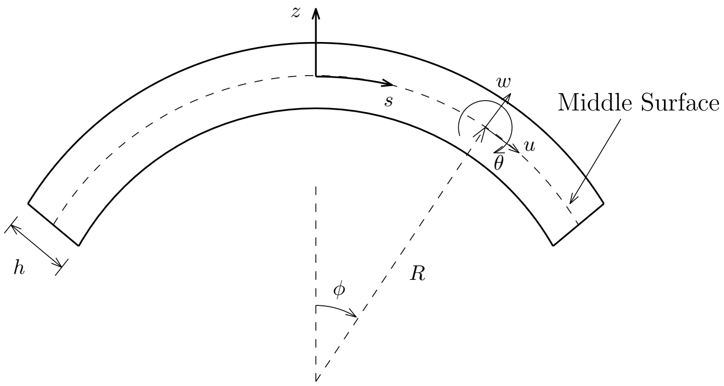


Figure 1. Thick curved beam element.

The extensional strain ($\varepsilon$), change of curvature ($\chi$) and the shear rotation ($\gamma$) are expressed in terms of the displacements and their derivatives by the following expressions:

$$\varepsilon = \frac{du}{ds} + \frac{w}{R}, \tag{1}$$

$$\chi = \frac{d\theta}{ds}, \tag{2}$$

$$\gamma = \theta + \frac{dw}{ds} - \frac{u}{R}, \tag{3}$$

where $R$ is the curvature radius.

The strain energy ($U$), the kinetic energy ($T$) and the work done by the external forces ($W$) expressions are:

$$U = \frac{1}{2}\int_0^{L_e} \left(E\,A\,\varepsilon^2 + E\,I\,\chi^2 + k\,G\,A\,\gamma^2\right)\,ds, \tag{4}$$

$$T = \frac{1}{2}\int_0^{L_e} \left(\rho\,A\,\dot{u}^2 + \rho\,A\,\dot{w}^2 + \rho\,I\,\dot{\theta}^2\right)\,ds, \tag{5}$$

$$W = \frac{1}{2}\int_0^{L_e} \left(p_\alpha\,u + p_n\,w + m_n\,\theta\right)\,ds, \tag{6}$$

where $E$ is the Young's modulus, $A$ is the cross-sectional area, $I$ is the moment of inertia, $\rho$ is the material density, $L_e$ is the element length, $k$ is the shear correction factor, $G$ is the shear modulus and $p_\alpha$, $p_n$, and $m_n$ are, respectively, the distributed tangential load, radial load and moment.

The displacement fields are describes as:

$$u = \mathbf{P}^T \cdot \mathbf{q}, \tag{7}$$

$$w = \mathbf{Q}^T \cdot \mathbf{q}, \tag{8}$$

$$\theta = \mathbf{J}^T \cdot \mathbf{q}, \tag{9}$$

where:

$$\mathbf{q} = \left\{ \begin{array}{ccc} \mathbf{u} & \mathbf{w} & \boldsymbol{\theta} \end{array} \right\}^T, \tag{10}$$

$$\mathbf{P} = \left\{ \begin{array}{ccc} \mathbf{P}^* & 0 & 0 \end{array} \right\}^T, \tag{11}$$

$$\mathbf{Q} = \left\{ \begin{array}{ccc} 0 & \mathbf{Q}^* & 0 \end{array} \right\}^T, \tag{12}$$

$$\mathbf{J} = \left\{ \begin{array}{ccc} 0 & 0 & \mathbf{J}^* \end{array} \right\}^T, \tag{13}$$

where $\mathbf{u}$, $\mathbf{w}$ and $\boldsymbol{\theta}$ are vectors containing, respectively, the degrees of freedom related to $u$, $w$ and $\theta$ and $\mathbf{P}^*$, $\mathbf{Q}^*$ and $\mathbf{J}^*$ are vectors containing, respectively, the shape functions related to $u$, $w$ and $\theta$.

The equations of motion can be derived by employing the Hamilton's principle:

$$\int_{t_0}^{t_1} \delta \left( U - T - W \right) dt = 0. \tag{14}$$

Through Eq. (14) the equation of motion are given by:

$$\mathbf{M}\,\ddot{\mathbf{q}} + \mathbf{K}\,\mathbf{q} = \mathbf{f}. \tag{15}$$

where the terms of the elementary mass matrix, elementary stiffness matrix and the force vector are:

$$K_{ij}^e = \int_0^{L_e} \left\{ \begin{array}{c} \dfrac{dP_i}{ds} + \dfrac{Q_i}{R} \\ \dfrac{dJ_i}{ds} \\ J_i + \dfrac{dQ_i}{ds} - \dfrac{P_i}{R} \end{array} \right\}^T \left[ \begin{array}{ccc} E\,A & 0 & 0 \\ 0 & E\,I & 0 \\ 0 & 0 & k\,G\,A \end{array} \right] \left\{ \begin{array}{c} \dfrac{dP_j}{ds} + \dfrac{Q_j}{R} \\ \dfrac{dJ_j}{ds} \\ J_j + \dfrac{dQ_j}{ds} - \dfrac{P_j}{R} \end{array} \right\} ds, \tag{16}$$

$$M_{ij}^e = \int_0^{L_e} \left\{ \begin{array}{c} P_i \\ Q_i \\ J_i \end{array} \right\}^T \left[ \begin{array}{ccc} \rho\,A & 0 & 0 \\ 0 & \rho\,A & 0 \\ 0 & 0 & \rho\,I \end{array} \right] \left\{ \begin{array}{c} P_j \\ Q_j \\ J_j \end{array} \right\} ds, \tag{17}$$

$$f_i^e = \int_0^{L_e} \left\{ \begin{array}{c} p_\alpha \\ p_n \\ m_n \end{array} \right\}^T \left\{ \begin{array}{c} P_i \\ Q_i \\ J_i \end{array} \right\} ds. \tag{18}$$

and $\ddot{q}$ is the generalized acceleration vector related to $u$, $w$ and $\theta$.

## 3 Generalized Finite Element Method

The GFEM is a Galerkin method with the main goal is to enrich the traditional FEM approximation space using previously knowledge about the solution in order to increase the precision of the approximated solution. The GFEM approximation space is obtained applying the Partition of Unity Method.

The approximated solution of a generic displacement field ($v$) can be written as the sum of two components:

$$v_h^e = v_{FEM}^e + v_{ENR}^e, \tag{19}$$

where:

$$v_{FEM}^e(\xi) = \sum_{i=1}^{2} \eta_i(\xi)\, a_i, \tag{20}$$

and

$$v^e_{ENR}(\xi) = \sum_{i=1}^{2} \eta_i(\xi) \left( \sum_{j=1}^{n} \phi_j(\xi)\, b_{ij} \right), \tag{21}$$

where $\eta(\xi)$ are the Partition of Unity functions, $a_i$ are the nodal degrees of freedom, $\phi_j(\xi)$ are the enrichment functions and $b_{ij}$ are the non nodal degrees of freedom.

In this paper, the linear Partition of Unity functions are used, which are in domain $[-1, 1]$:

$$\eta_1(\xi) = \frac{1-\xi}{2} \tag{22}$$

and

$$\eta_2(\xi) = \frac{1+\xi}{2}, \tag{23}$$

with $\xi = \frac{2\,s}{L_e} - 1$.

The enrichment functions used are based on Leung and Zhu [13], and are given by the following expression:

$$\phi_j(\xi) = \sin\left[ j\,\pi \left( \frac{\xi+1}{2} \right) \right] \quad \text{with} \quad j \geq 1. \tag{24}$$

It is important to highlight that although the enrichment functions used in this work are the same employed by Leung and Zhu [13] in $p$-Fourier curved beam elements, the GFEM elements proposed here use the partition of unity technique (Eq. (21)) resulting in an enrichment different from those proposed by [13].

All the three displacement fields cited in previously section ($u$, $w$ and $\theta$) are described by the approach proposed in this section to construct the GFEM approximation.

## 4 Numerical Results

In this section two examples of thick curved beams are analyzed: a pinned-pinned arch and a clamped-clamped arch. In order to evaluate the performance of the GFEM proposed, modal and transient analyses are made.

The modal analysis results are compared to reference solutions found in the literature and the transient analysis results are compared to a reference FEM model that has the same formulation of the GFEM model, but without the $v^e_{ERN}$ component (Eq. (21)) and a higher number of degrees of freedom. In transient analysis the two examples have the same load ($P(t)$) given by:

$$P(t) = 10000\, \sin(10\, t), \tag{25}$$

with time ($t$) in seconds and the load ($P(t)$) in Newton.

For the time integration the Newmark method with constant acceleration and time step of 0.0001 seconds are used.

### 4.1 Pinned-Pinned Arch

The arch studied here has the load applied in the middle of the arch in radial direction, as shown in Fig. 2. The arch has the Young's module of 70 GPa, curvature radius of 0.75 m, cross section area of 4 m$^2$, inertia moment of 0.01 m$^4$, shear correction factor of 0.85, material density of 2777 kg/m$^3$ and Poisson coefficient of 0.3.

The first analysis is a modal analysis, without load. The results are compared to those found in Einsenberger and Efraim [22] and Yang et al. [21] and are presented in function of the adimensional parameter, given by:

$$C_n = \omega_n\, R \sqrt{\frac{\rho\, A}{E\, I}}, \tag{26}$$

where $\omega_n$ is the frequency obtained in model, $R$ is the curvature radius, $\rho$ is the material density, $A$ is the cross section area, $E$ is the Young's module and $I$ is the inertia moment.

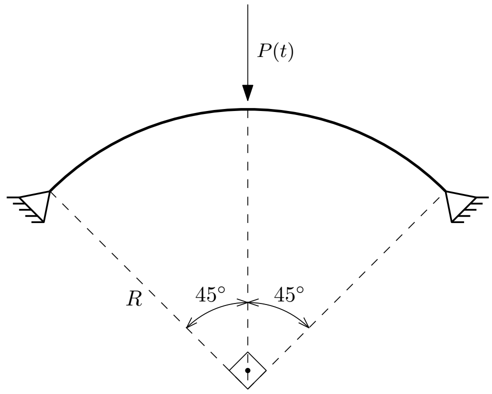


Figure 2. Pinned-Pinned arch scheme.

All the GFEM models analyzed have only one finite element and increasing number of enrichment levels are increases. The results are presented in Table 1.

Table 1. Adimensional parameters of pinned-pinned arch.

| Mode | GFEM | | | | Ref 1* | Ref 2** |
|---|---|---|---|---|---|---|
| | 2 levels 18 d.o.f. | 4 levels 30 d.o.f. | 6 levels 42 d.o.f. | 8 levels 54 d.o.f. | | |
| 1 | 29.37551 | 29.27996 | 29.27990 | 29.27990 | 29.280 | 29.304 |
| 2 | 33.30563 | 33.30493 | 33.30492 | 33.30492 | 33.305 | 33.243 |
| 3 | 68.83937 | 67.12352 | 67.12352 | 67.12352 | 67.124 | 67.123 |
| 4 | 80.47276 | 79.97083 | 79.97081 | 79.97081 | 79.971 | 79.950 |
| 5 | 133.59291 | 107.85168 | 107.85111 | 107.85111 | 107.851 | 107.844 |
| 6 | 152.47795 | 143.66392 | 143.61754 | 143.61754 | 143.618 | 143.679 |
| 7 | 227.73503 | 156.78591 | 156.66557 | 156.66557 | 156.666 | 156.629 |
| 8 | 304.81366 | 193.55645 | 190.47711 | 190.47709 | 190.477 | 190.596 |
| 9 | 312.86477 | 225.86638 | 225.36120 | 225.36115 | 225.361 | 225.349 |
| 10 | 321.77082 | 280.13587 | 234.53334 | 234.52351 | 234.524 | 234.809 |

**Note:** * - Einsenberger and Efraim [22] and ** - Yang et al. [21].

The GFEM modal analysis shows good agreement with the references solutions of Einsenberger and Efraim [22] and Yang et al. [21].

The next analysis performed is the transient analysis with the external load as described in Eq. (25). Now the GFEM model has only two finite elements and six enrichment levels, resulting in 81 degrees of freedom. The reference FEM model has 400 finite elements, resulting in 1203 degrees of freedom. The results are presented in Fig. 3, 4 and 5 in terms of displacements, velocity and acceleration, respectively, all three in radial direction in the middle point of the arch.

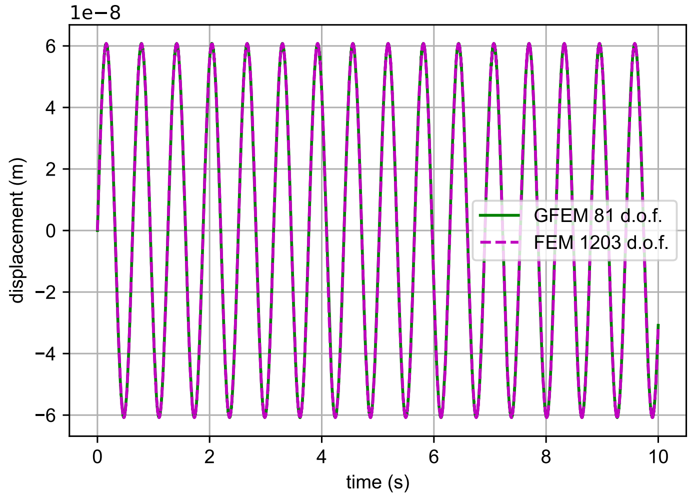


Figure 3. Pinned-Pinned Arch displacement.

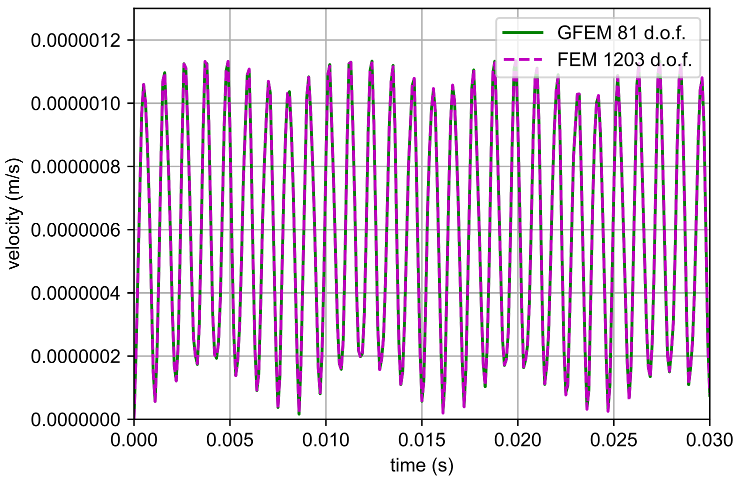


Figure 4. Pinned-Pinned Arch velocity.

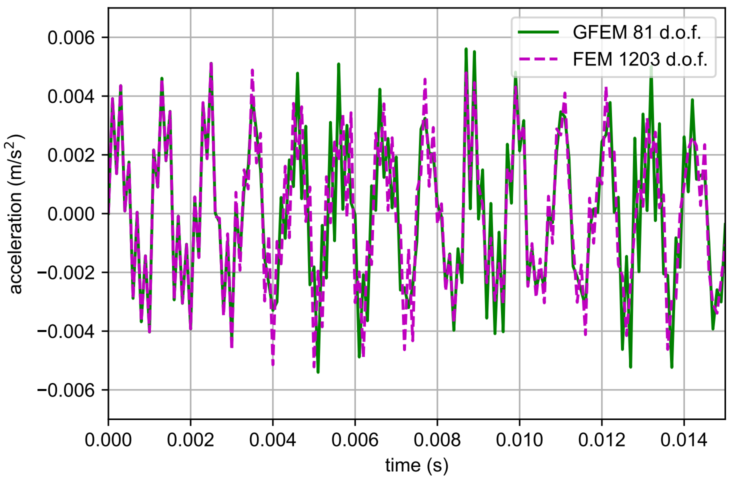


Figure 5. Pinned-Pinned Arch acceleration.

The GFEM results show good agreement for displacement and velocity compared to the reference FEM solution, with much less degrees of freedom. But the GFEM acceleration results present some differences compared to with FEM results.

### 4.2 Clamped-clamped arch

The arch studied here also has the load applied in the middle of the arch in radial direction, as shown in Fig. 6. The arch has the Young's module of 70 GPa, curvature radius of 0.6366 m, cross section area of 1 $m^2$, inertia moment of 0.0016 $m^4$, shear correction factor of 0.85, material density of 2777 $kg/m^3$ and Poisson coefficient of 0.3.

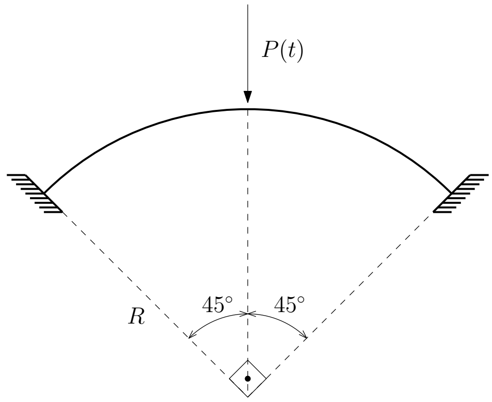


Figure 6. Clamped-clamped arch scheme.

The first analysis is a modal analysis, without load. The results are also compared with those found in Einsenberger and Efraim [22] and Yang et al. [21] and are presented in function of the adimensional parameter, Eq. (26).

All the GFEM models analyzed have only one finite element and increasing number of enrichment levels are increases. The results are presented in Table 2.

Such as the previous example, the results present good agreement with references solutions of Einsenberger and Efraim [22] and Yang et al. [21].

The next analysis is the transient analysis also with the external load as described in Eq. (25). The GFEM model has only two finite elements and six enrichment levels, resulting in 81 degrees of freedom. The FEM model has 400 finite elements, resulting in 1203 degrees of freedom. The results are presented in Fig. 7, 8 and 9 in terms of displacements, velocity and acceleration, respectively, all three in radial direction in the middle point of the arch.

The GFEM results shows goods agreement for displacement and velocity compared to the FEM reference solution, with much less degrees of freedom. But the GFEM acceleration results presented some differences compared to FEM reference solution, such as in the pinned-pinned example.

## 5 Conclusion

In this paper the application of GFEM for dynamic, modal and transient, analysis of thick curved beams was presented. A generalized element for thick curved beam was proposed using trigonometric functions as enrichment functions.

Both examples presented good agreement with references results for modal analysis, as shown in Tables 1 and 2. In transient analysis the results were very satisfactory for displacement and velocity, with much less degrees of freedom compared to implemented FEM reference, but the accelerations results were not so satisfactory.

In general, for the first application of GFEM for thick curved beams, the results are satisfactory, demonstrating the potential of the GFEM in dynamics analysis of thick curved beams.

Table 2. Adimensional parameters of clamped-clamped arch.

| Mode | GFEM | | | | Ref 1* | Ref 2** |
|---|---|---|---|---|---|---|
| | 2 levels 18 d.o.f. | 4 levels 30 d.o.f. | 6 levels 42 d.o.f. | 8 levels 54 d.o.f. | | |
| 1 | 36.72935 | 36.70221 | 36.70219 | 36.70219 | 36.703 | 36.657 |
| 2 | 42.41161 | 42.26315 | 42.26293 | 42.26293 | 42.264 | 42.289 |
| 3 | 85.20288 | 82.23165 | 82.23159 | 82.23159 | 82.233 | 82.228 |
| 4 | 90.86340 | 84.48906 | 84.48904 | 84.48904 | 84.491 | 84.471 |
| 5 | 161.84674 | 122.30335 | 122.30289 | 122.30289 | 122.305 | 122.298 |
| 6 | 167.23451 | 155.01386 | 154.94066 | 154.94066 | 154.945 | 154.998 |
| 7 | 241.63618 | 168.52165 | 168.19834 | 168.19834 | 168.203 | 168.174 |
| 8 | 338.73814 | 208.88817 | 204.46725 | 204.46723 | 204.472 | 204.599 |
| 9 | 354.41808 | 239.53494 | 238.98475 | 238.98467 | 238.992 | 238.973 |
| 10 | 384.12593 | 300.96222 | 249.02336 | 249.00551 | 249.011 | 249.320 |

**Note:** * - Einsenberger and Efraim [22] and ** - Yang et al. [21].

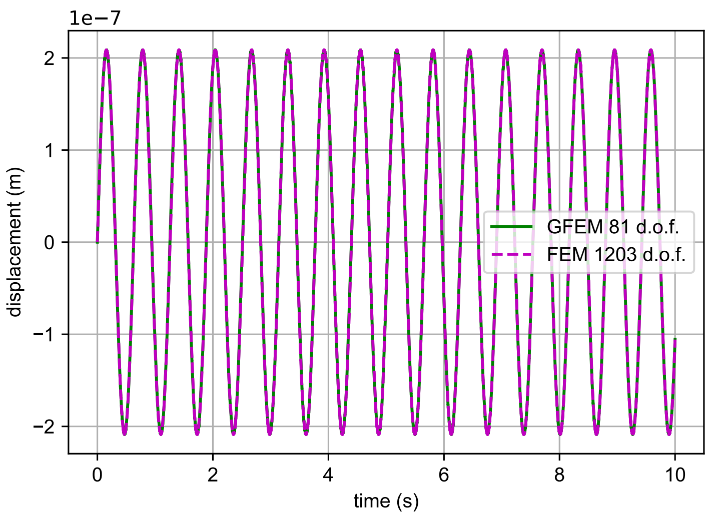


Figure 7. Clamped-clamped Arch displacement.

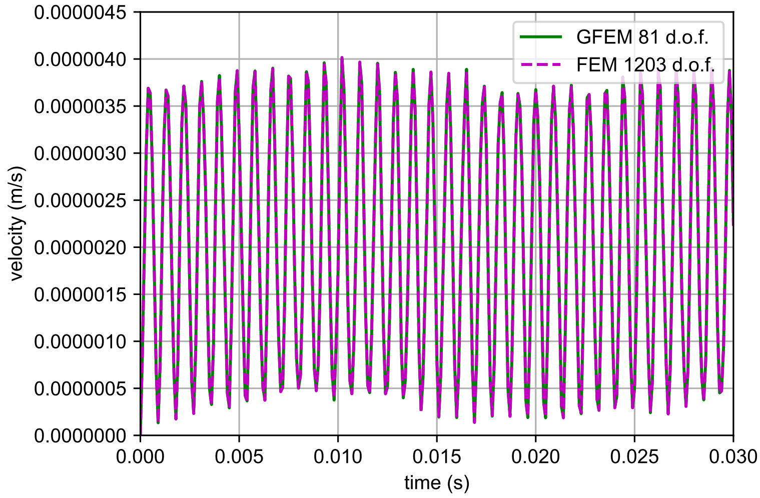


Figure 8. Clamped-clamped Arch velocity.

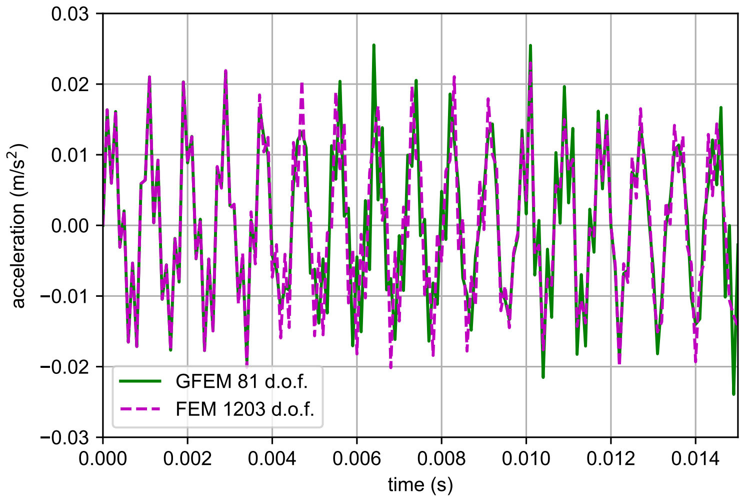


Figure 9. Clamped-clamped Arch acceleration.

## Acknowledgements

The authors respectfully acknowledge CAPES and CNPq for the financial support.

## References

[1] M. Arndt, R. D. Machado, and A. Scremin. An adaptive generalized finite element method applied to free vibration analysis of straight bars and trusses. *Journal of Sound and Vibration*, vol. 329, n. 6, pp. 659–672, 2010.

[2] A. Y. T. Leung and J. K. W. Chan. Fourier p-element for the analysis of beam and plates. *Journal of Sound and Vibration*, vol. 212, n. 1, pp. 179–185, 1998.

[3] P. Ribeiro. Hierarchical Finite Element Analyses of Geometrically Non-Linear Vibration of Beams and Plane Frames. *Journal of Sound and Vibration*, vol. 246, n. 2, pp. 225–244, 2001.

[4] J. M. Melenk and I. Babuska. The partition of unity finite element method: Basic theory and applications. *Computer Methods in Applied Mechanics and Engineering*, vol. 139, pp. 289–314, 1996.

[5] C. A. M. Duarte and J. T. Oden. An h-p adaptive method using clouds. *Computer Methods in Applied Mechanics and Engineering*, vol. 139, pp. 237–262, 1996.

[6] J. T. Oden, C. A. M. Duarte, and O. C. Zienkiewicz. A new cloud-based hp finite element method. *Computer Methods in Applied Mechanics and Engineering*, vol. 153, pp. 117–126, 1998.

[7] C. A. M. Duarte, I. Babuska, and J. T. Oden. Generalized finite element methods for three-dimensional structural mechanics problems. *Computers and Structures*, vol. 77, pp. 215–232, 2000.

[8] I. Babuska, U. Banerjee, and J. E. Osborn. Generalized finite element methods: main ideas, results, and perspective. *International Journal of Computational Methods*, vol. 1, n. 67, pp. 67–103, 2004.

[9] M. Arndt, R. D. Machado, and A. Scremin. Accurate assessment of natural frequencies for uniform and non-uniform euler-bernoulli beams and frames by adaptive generalized finite element method. *Engineering Computations*, vol. 33, n. 5, pp. 1586–1609, 2016.

[10] A. J. Torii and R. D. Machado. Structural dynamic analysis for time response of bars and trusses using the generalized finite element method. *Latin American Journal of Solids and Structures*, vol. 9, n. 3, pp. 1–31, 2012.

[11] H. Y. Shang, R. D. Machado, and J. E. Abdalla Filho. Dynamic analysis of euler–bernoulli beam problems using the generalized finite element method. *Computers and Structures*, vol. 173, pp. 109–122, 2016.

[12] P. O. Weinhardt, L. B. C. Debella, M. Arndt, and R. D. Machado. Gfem stabilization techniques applied to dynamic analysis of non-uniform section bars. *Latin American Journal of Solids and Structures*, vol. 15, n. 11, pp. 64–84, 2018.

[13] A. Y. T. Leung and B. Zhu. Fourier p-elements for curved beam vibrations. *Thin-Walled Structures*, vol. 42, pp. 39–57, 2004.

[14] M. Petyt and C. C. Fleischer. Free vibration of a curved beam. *Journal of Sound and Vibration*, vol. 18, n. 1, pp. 1–30, 1971.

[15] D. J. Dawe. Numerical studies using circular arch finite elements. *Computers and Structures*, vol. 4, pp. 729–740, 1974.

[16] R. Raveendranath, G. Singh, and B. Pradhan. A two-noded locking-free shear flexible curved beam element. *International Journal for Numerical Methods in Engineering*, vol. 44, pp. 265–280, 1999.

[17] R. E. Rossi and P. A. A. Laura. Dynamic stiffening of an arch clamped at one end and free at the other. *Journal of Sound and Vibration*, vol. 160, pp. 190–192, 1993.

[18] N. M. Auciello and M. A. De Rosa. Free vibrations of circular arches: a review. *Journal of Sound and Vibration*, vol. 4, n. 176, pp. 433–458, 1994.

[19] R. Raveendranath, G. Singh, and B. Pradhan. Free vibration of arches using a curved beam element based on a coupled polynomial displacement. *Computers and Structures*, vol. 78, pp. 583–590, 2000.

[20] R. Raveendranath, G. Singh, and G. V. Rao. A three-noded shear-flexible curved beam element based on coupled displacement field interpolations. *Journal for Numerical Methods in Engineering*, vol. 51, pp. 85–101, 2001.

[21] F. Yang, R. Sedaghati, and E. Esmailzadeh. Free in-plane vibration of general curved beams using finite element method. *Journal of Sound and Vibration*, vol. 318, pp. 850–867, 2008.

[22] M. Einsenberger and E. Efraim. In-plane vibrations of shear deformable curved beams. *International Journal for Numerical Methods in Engineering*, vol. 52, pp. 1221–1234, 2001.